ChemComm

Accepted Manuscript

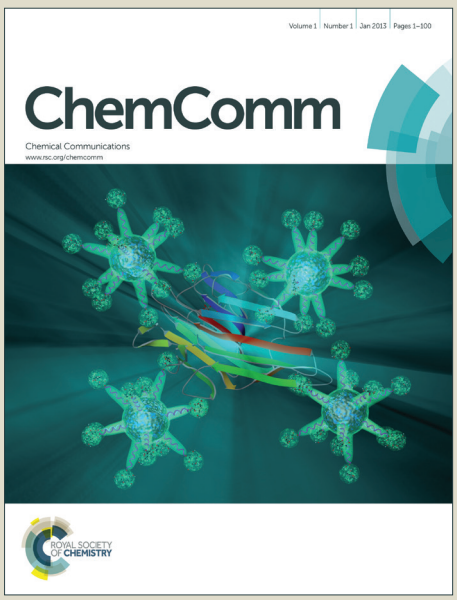

ROYAL SOCIETY OF CHEMISTRY

www.rsc.org/chemcomm

Cite this: DOI: 10.1039/coxx00000x

www.rsc.org/xxxxxx

ARTICLE TYPE

Stimuli Responsive Chiral Liquid Crystal Phases of Phenylboronic Acid Functionalized Rodlike Viruses and Their Interaction with Biologically Important Diols

Jun Cao,[a,b] Shuaiyu Liu,[a,b] Jie Xiong, [a,b] Yingjun Chen, [a,b] and Zhenkun Zhang* [a,b]

Received (in XXX, XXX) Xth XXXXXXXXX 20XX, Accepted Xth XXXXXXXXX 20XX
DOI: 10.1039/b000000x

The rodlike M13 virus with chemically decorated phenylboronic acid moieties forms pH responsive chiral nematic liquid crystal (LC) phases. Binding with biological important diols results in LC phases with microstructures that closely correlate with the molecular structure of the diols and can be conveniently discerned by visual cues.

Viruses recently have attracted tremendous interest in versatile fields ranging from nanomaterials, biomedicines to fundamental research. Such versatility is due to their genetic and chemical addressability, nanoscale size and defined spherical or rodlike shape.[1] Genetically and chemically modified viruses have found applications in many fields.[2] Rodlike viruses are also ideal building blocks for lyotropic liquid crystal (LC) materials due to their monodisperse and anisotropic shape.[3] Most of rodlike particles normally form nematic LC phases, in which the long axis of the rodlike particles point to one direction while no positional ordering exists. However, the prestigious feature of the rodlike viruses is that some of them, such as the M13, fd virus, can form chiral nematic LC (CLC) phases.[3a, f] In such a phase, the long axis of the rodlike virus arranges in a helical way around a director, resulting in stripe-like fingerprints. The periodicity of the fingerprints is in the micrometer range and can be conveniently observed by polarized optical microscopy (POM) (Figure 1B). This is an elegant example from nature that three dimensional hierarchal self-assembled structures can be achieved by subtle inter-particle interactions and has fascinated researchers from various fields. Compared to their small molecular counterparts that have been widely used in many fields such as display technology, sensors, optical materials, etc,[4] lyotropic liquid crystal (LC) formed by rodlike nanocolloidal particles is limited. Especially, in the case of rodlike viruses, although understanding of the physical origin of their CLC phase have advanced greatly,[3f, 5] how to wisely use such phases lags behind. [6]

Herein, we present a stimuli responsive chiral nematic LC system based on the rodlike virus–M13 bacteriophage modified with phenylboronic acid (PBA) moieties. We further exploit the dynamic LC response to specific binding with biological important diols, which manifests as simple visual cues. The M13 virus, a natural nanorod with a length of 880 nm and a diameter of 6.6 nm, is basically a rodlike protein capsid consisting of ca. 2700 coat proteins (P8) in which the viral gene was wrapped.[7] On the surface of M13, ca.5400 amino groups of the Lys 8 and *N*-terminal arrange with nanoscale precision on the virus surface and offer tremendous opportunities for chemical modifications.[2] PBA is pH sensitive and can transform between the hydrophobic neutral trigonal form and hydrophilic tetrahedral boronate anion through tuning the environmental pH lower or above its p*K*a (Figure 1).[8] We conjecture that the pH-dependent amphiphilicity of PBA moieties on the surface of the M13 virus can be exploited to fine-tune the 3D arrangement of the viral particles in the nematic LC phase. Furthermore, boronic acid can form reversible, dynamic covalent bonds with compounds containing the cis-1,2 and cis-1,3 diol groups, such as saccharides. There are tremendous applications in sensors based on such high affinity of boronic acids toward polyols, which generally relies on either fluorescent or conductivity changes upon binding of diols with a boronic acid moiety. [9, 15]

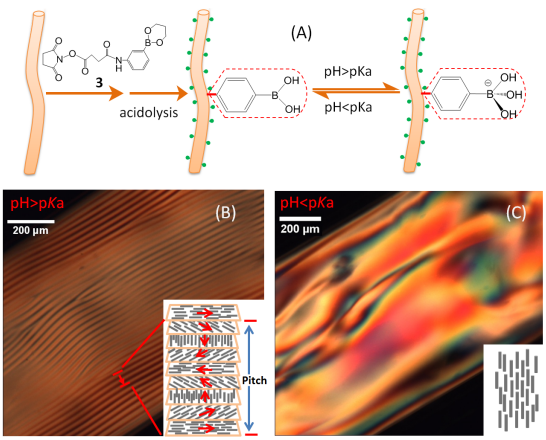

Fig. 1 (A) Schematic representation of the chemical modification of the rodlike M13 virus with an *N*-hydroxysuccinimide ester (NHS) derivative of phenylboronic acid (**3**). (B) and (C) pH dependent liquid crystal behaviour of M13-PBA. The chiral nematic LC phase (B) was formed at pH = 10.2 (200 mM carbonate buffer) while the pure nematic LC phase (C) was formed at pH = 7.2 (100 mM phosphate buffer). The concentration of M13-PBA is 30 mg mL^{-1}. Insets: schematic representation of the 3D ordering of the rodlike virus in each phase.

For our purpose, an *N*-hydroxysuccinimide ester (NHS) derivatives-DDPCP (**3** in Figure 1), was synthesized and coupled to the virus surface under mild conditions (Figure 1A, see ESI for the details†).[10] It is well established that coupling of such

compounds only occur to the surface amino groups of the virus due to the compact packing of the coat protein in the capsid.[2b, g] MALDI-TOF mass spectroscopy analysis confirmed that part of the coat proteins was coupled with PBA (Figure S3 in ESI†). Around 700 PBA groups are installed on each virus. Atomic force microscopy (AFM) and transmission electronic microscopy (TEM) revealed the rodlike conformation of the modified viruses (Figure S6 in ESI†). From dynamic light scattering (DLS), the M13-PBA hybrid virus has an apparent hydrodynamic diameter (D_h) distribution similar with the pristine M13 virus under the conditions where the PBA moieties are either in the hydrophobic state or in the hydrophilic state (Figure S5†). This result indicates that the M13-PBA virus is still colloidally stable and no inter-virus aggregation exists in aqueous media. Such excellent colloidal stability stems from the negative surface charges offered by the large amount of carboxyl groups (See Table S1 in ESI for the apparent zeta potential of the viruses†).[11] In addition, M13-PBA and pristine M13 viruses have similar circular dichroism (CD) spectrum and endogenous fluoresce behaviors of the Try26 of the P8 coat protein (Figure S4†).[12] Therefore, coupling PBA to part of the coating protein does not perturb the helical structure of the coat proteins and their helical packing in the capsid. This is important since such factors are known to influence the nature of the nematic LC phase of the filamentous viruses.[5] Finally, the solvent exposure and specific binding capability of the viral surface PBA moieties to diols were confirmed by the standard fluorogentic method based on Alizarin red S (ARS). ARS turns from the non-fluorescent into fluorescent state after binding with PBA moieties (Figure S7†).[13] The apparent binding constant, $K_{b,app}$, of the PBA groups on the virus surface to several typical diol compounds was estimated following literature methods (Table S1).[13] The different affinity to the various diols is consistent with literature but $K_{b,app}$ is much higher than that of free PBA and diols under the same conditions.[13]

Similar to unmodified M13, the M13-PBA suspended in aqueous buffer turned from the isotropic into nematic LC phase above certain threshold concentration. The concentration range is comparable to the unmodified M13 in the same buffer (Table S1†), indicating that M13-PBA and M13 have similar physical properties such as flexibility and surface charge.[3f, 5] However, the 3D ordering the virus in the nematic LC phase of M13-PBA strictly depends on the environmental pH. At pH < p*K*a of the PBA (ca. 8.9), M13-PBA only formed pure nematic LC phase (Figure 1C). At pH > p*K*a, the classic fingerprint of the CLC phase recovered (Figure 1A), and the CLC phase exists in the whole virus concentration range of the nematic LC phase. It is noted here that the pristine M13 virus formed the CLC in the same buffers, consistent with previous results.[3g] All the results so far point to the fact that M13-PBA and unmodified M13 have similar secondary structure of the coat proteins, packing style of the capsid, flexibility and surface charges, which are factors known to influence the nature of the nematic LC phase of M13.[5] Therefore, the pH dependent nematic LC phase of M13-PBA must be due to the coupled PBA moieties. The PBA moieties are hydrophobic when pH < p*K*a.[8] While the virus can still be kept colloidally stable due to the electrostatic repulsion of the large amount of surface carboxyl groups as indicated by DLS (Figure S5), hydrophobic PBA moieties probably confer attractive interactions among the M13-PBA viruses. Such interaction may favor the tendency of intervirus parallel in order to maximize the attraction, leading to the formation of the pure nematic phase. It is noted here that the attraction brought by the PBA moieties is not strong enough to induce gelation at such high concentrations for the LC phase as indicated by the liquid-like rheological behavior of the concentrated M13-PBA suspension (Figure S8†). When pH > p*K*a, the PBA moieties become hydrophilic and charged, intervirus repulsion is the dominant interaction which helps the formation of the CLC phase. To the best of our knowledge, this is the first example that has pH responsive reconfigurable 3D arrangement of rodlike particles in the nematic LC phase.

As stated before, boronic acid is the classic receptor for diol containing compounds. The above results also highlight the sensitivity of the microstructure of the nematic LC phase to the chemical state of PBA moieties in the case of M13-PBA. We conjecture that diol compounds of various molecular structures may induce different intervirus interactions after binding to the surface PBA groups. Such binding may result in LC phases with a microstructure that closely correlate with the molecular structure of the diols and can be conveniently discerned by POM or naked eyes. As a prove of concept, two classes of biologically important diols were tested: i) aromatic diols such as catechol and its derivates, which are 1,2-dihydroxyphenyl containing compounds (See Scheme S3 in ESI†); ii) aliphatic diols such as glucose and fructose, two typical monosaccharides. The pH was kept above the p*K*a where M13-PBA will form perfect CLC phase (Figure 1B). In the presence of enough amount of aromatic diols (above ca. 40 μM), the perfect CLC phase of the M13-PBA was completely quenched and only pure nematic LC phases formed, regardless of the chemical structure of the diols (Figure 2 and S9†). As a control, unmodified M13 was mixed with the same amount of aromatic diols under identical conditions and the CLC phase always formed. DLS also revealed no inter-virus aggregation existed as indicated by the similar hydrodynamic diameter distribution between the M13, M13-PBA in the absence or presence of catechol (Figure S5C, D†), excluding the possibility that the pure nematic LC phase may stem from catechol induced aggregation. Therefore, the pure nematic LC phase in the presence of catechol derivatives must be due to the subtle intervirus interactions brought by binding of the aromatic diols to BPA receptors on the virus surface. With synperi-planar arrangement of the aromatic hydroxyl groups and their electro-donating character, catechol and derivatives can easily react with boronic acid moiety, resulting in five membered cyclic esters linked to two aromatic benzene rings (Figure 2A). Probably, such aromatic dominant groups may bring hydrophobic, or π-π stacking into the intervirus interactions which favor the formation of pure nematic LC phase.

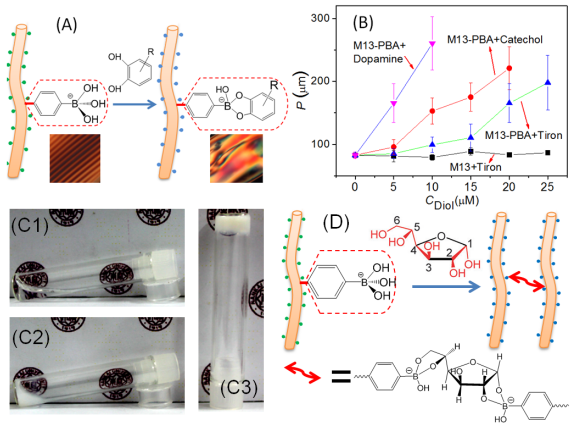

Fig. 2 Solution behavior of M13-PBA in the presence of diols. (A) Schematic representation of the binding of catechol and derivatives with PBA moieties on the surface of the M13 virus. (B) Influence of the amount of catechol and derivatives on the pitch of the CLC phase of M13-PBA. The buffer and the concentration of M13-PBA are the same as in Figure 1B. Dihydroxybenzene(catechol), dopamine, and 4,5-dihydroxy-1,3-bezenedisulfonate(Tiron) were investigated (See Scheme S3† for the chemical structure of these diols). (C) Photos of the three states of M13-PBA suspension in the presence of glucose: transparent (C1), opaque suspension (C2) or gel (C3). (D) Schematic illustration of the intervirus crosslinking by the furansoe form of D-glucose.

The 3D arrangement of the M13-PBA in the nematic LC phase is indeed very sensitive to the amount of catechol and its derivatives. Although the CLC phase can still form in the M13-PBA suspension in the presence of a small amount of catechol and derivatives such as 5 μM Tiron, the fingerprint textures is less regular compared to that of pure M13-PBA (Fig. S9 in ESI†). With increasing amount of catechol, the homogeneity of the CLC phase further decreased with increasing areas corresponding to the pure nematic LC phase (Fig. S9 in ESI†). The twist periodicity of rodlike viruses in the CLC phase was characterized by the cholesteric pitch (*P*) (Highlighted in Figure 1B). Under otherwise identical conditions, smaller pitch means stronger tendency to form the CLC phase and vice versa. As listed in Fig. 2B, it is clear that, with increasing amount of diols, the pitch of the CLC phase also increased, suggesting unwinding of the helically ordered rodlike viruses. Among the three aromatic diols, the power of quenching the CLC phase follows the order of dopamine > catechol > Tiron. Above 10 μM dopamine, the inhomogeneity approaches such a degree that determination of the pitch is impossible. Such specific power of dopamine might be relative to its chemical structure (Scheme S3†). Besides the binding of the 1,2-dihydroxyphenyl moieties with the surface coupled PBA, the amino group of dopamine can electrostaticly interact with the rich surface carboxyl groups of the virus.[14] This effect will further complicate intervirus interactions that facilitate the formation of the pure nematic LC phase. Tiron has two anionic sulfonate groups which might counteract the attractive interaction brought by the aromatic benzene rings. Therefore, Tiron has the lowest efficacy to quench the CLC phase of M13-PBA. The general trend is that reagents, if containing aromatic moieties and/or groups which can interact with the virus surface to introduce subtle attractive interactions, have stronger power to induce change in the phase behaviour of the virus.

In contrast to the aromatic diols, in the presence of monosaccharides such as fructose, the M13-PBA can still form perfect CLC phases, regardless of the amount of the added sugar. This can be ascribed to the hydrophilicity of boronate ester formed by binding the monosaccharide to PBA (Scheme S2 in ESI†). Glucose is expected to follow the same trend of fructose. However, in the presence of glucose, the M13-PBA suspension turned into opaque suspension or gel, depending on the relative ratio of the glucose to the M13-PBA (Fig. 2C, D and S10A†). It is known that the furanose form of the monosaccharides is favored by the binding with boronic acids (Fig. S2B in ESI†). The furanose form of D-glucose, α-D-glucofuranose, has a pair of *cis*-diol units in the 1,2- and 5,6-positions which act as two binging sites and render glucose with the unique property to form 1:2 complex with boronic acids (Fig. S2B in ESI †).[15] Therefore, the glucose molecule can covalently react with two PBA moieties from two viruses and crosslinking them together (inter-virus crosslinking), as indicated by bundles of several viruses (Fig. S10B in ESI†). In addition, the linear polymer like conformation of the semi-flexible rodlike virus can facilitate such crosslinking. Therefore, by visual investigation of the nature of the nematic phase formed by the M13-PBA in the presence of different kinds of diols, one can discriminate between aromatic diols such as catechol derivates and aliphatic monosaccharides. The distinct solution behavior of M13-PBA in the presence of fructose and glucose might help selective sensing of glucose over fructose.

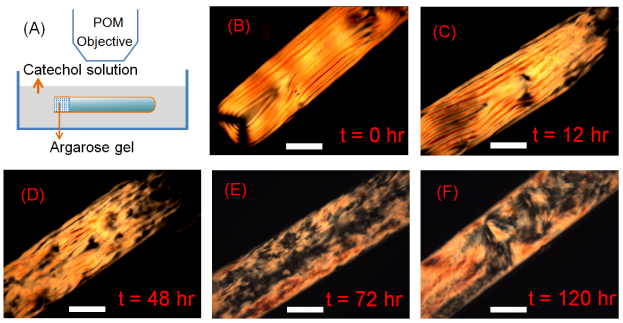

Fig.3 (A) Schematic illustration of a prototype device to monitor the fingerprint texture change of the cholesteric LC phase of M13-PBA under the influence of catechol. (B) ~ (F) Typical texture of the nematic LC phase of M13-PBA recorded at the noted time. The M13-PBA was filled in a glass capillary which was immerged into a carbonate buffer containing 40 μM catechol. Scale bar: 500 μm.

Finally, to demonstrate potential applications, a simple device was designed to visualize the interaction of catechol derivates with the surface BPA moieties by monitoring the fingerprint texture of the CLC phase of M13-PBA (Fig. 3). Concentrated M13-PBA was sealed in a glass capillary, in which the perfect chiral cholesteric LC phase formed. The open end of the capillary was blocked with a 3.0 % agar gel which allowed small molecules like diols to diffuse through freely while the virus was blocked. The capillary was immerged into aqueous buffer containing diols such as dopamine and the fingerprint texture of the CLC phase was monitored by POM (Fig. 3A). Upon diffusing of the diols inside the capillary, the cholesteric LC phase slowly became irregular start from the interface close to the gel at the time scale of several days. Eventually, the fingerprint texture in the whole capillary disappeared completely. When a similar capillary was immerged into the same aqueous buffer containing no any diol, no change occurred to the fingerprint texture (Fig. S11 in ESI†).

In conclusion, we prepared a phenylboronic acid (PBA) decorated M13 virus by convenient surface chemical modifications. The M13-PBA hybrid virus can form either pure nematic or chiral LC (CLC) phase, due to the pH-dependent amphiphilicity of PBA. Under the conditions suitable for the formation of the CLC phase, aromatic diols such as catechol, dopamine etc, can further influence the 3D ordering of the hybrid virus and induce the formation of the pure nematic LC phase. In contrast, monosaccharides such as fructose do not interfere with the formation of the chiral LC phase of the M13-PBA. Such responsive arrangement of the rodlike virus in the presence of varied diols might be found applications in the development of sensing materials.

Acknowledgements

This work was supported by the National Natural Science Foundation of China (No. 21274067, 91127045, 51390011), the Fundamental Research Funds for the Central Universities, Natural Science Foundation of Tianjin, China (No. 12JCQNJC01800) and PCSIRT (IRT1257). We would like to thank Prof. Linqi Shi for his generous supporting.

Notes and references

[a] *Key Laboratory of Functional Polymer Materials of Ministry of Education, and Institute of Polymer Chemistry, Nankai University, Tianjin, 300071, China; E-mail: zkzhang@nankai.edu.cn*

[b] *Collaborative Innovation Center of Chemical Science and Engineering(Tianjin), Tianjin 300072, China.*

† Electronic Supplementary Information (ESI) available: Materials, synthetic procedures, characterization and many other results.. See DOI: 10.1039/b000000x/

1 (a) W.-J. Chung, A. Merzlyak, S.-W. Lee, *Soft Matter* 2010, **6**, 4454-4459; (b) D. Ghosh, Y. Lee, S. Thomas, A. G. Kohli, D. S. Yun, A. M. Belcher, K. A. Kelly, *Nat. Nanotechnol.* 2012, **7**, 677-682; (c) T. Gibaud, E. Barry, M. J. Zakhary, M. Henglin, A. Ward, Y. Yang, C. Berciu, R. Oldenbourg, M. F. Hagan, D. Nicastro, *Nature* 2012, **481**, 348-351; (d) C. Mao, D. J. Solis, B. D. Reiss, S. T. Kottmann, R. Y. Sweeney, A. Hayhurst, G. Georgiou, B. Iverson, A. M. Belcher, Science 2004, 303, 213-217; (e) N. Gandra, D. D. Wang, Y. Zhu, C. Mao, *Angew. Chem., Int. Ed.* 2013, **125**, 11488-11491; (f) R. J. Tseng, C. Tsai, L. Ma, J. Ouyang, C. S. Ozkan, Y. Yang, *Nat. Nanotechnol.* 2006, **1**, 72-77.

2 (a) F. C. Wu, H. Zhang, Q. Zhou, M. Wu, Z. Ballard, Y. Tian, J. Y. Wang, Z. W. Niu, Y. Huang, *Chem. Commun*., 2014, **50**, 4007—4009; (b) K. Li, Y. Chen, S. Li, H. G. Nguyen, Z. Niu, S. You, C. M. Mello, X. Lu, Q. Wang, *Bioconjugate Chem.* 2010, **21**, 1369-1377; (c) Y. S. Nam, T. Shin, H. Park, A. P. Magyar, K. Choi, G. Fantner, K. A. Nelson, A. M. Belcher, *J. Am. Chem. Soc.* 2010, **132**, 1462-1463; (d) J. K. Pokorski, K. Breitenkamp, L. O. Liepold, S. Qazi, M. Finn, *J. Am. Chem. Soc*. 2011, **133**, 9242-9245; (e) Z. M. Carrico, M. E. Farkas, Y. Zhou, S. C. Hsiao, J. D. Marks, H. Chokhawala, D. S. Clark, M. B. Francis, *ACS Nano* 2012, **6**, 6675-6680; (f) Z. Zhang, J. Buitenhuis, A. Cukkemane, M. Brocker, M. Bott, J. K. Dhont, *Langmuir* 2010, **26**, 10593-10599.

3 (a) Z. Dogic, S. Fraden, *Langmuir* 2000, **16**, 7820-7824; (b) J. Lapointe, D. Marvin, *Mol. Cryst. Liq. Cryst*. 1973, **19**, 269-278; (c) R. Oldenbourg, X. Wen, R. Meyer, D. Caspar, *Phys. Rev. Lett.* 1988, **61**, 1851; (d) Z. Dogic, S. Fraden, *Phys. Rev. Lett.* 1997, **78**, 2417; (e) E. Grelet, *Phys. Rev. Lett.* 2008, **100**, 168301. (f) E. Grelet, S. Fraden, *Phys. Rev. Lett.* 2003, **90**, 198302; (g) K. R. Purdy, S. Fraden, *Phys. Rev. E* 2004, **70**, 061703.

4 (a) N. Tamaoki, *Adv. Mater.* 2001, **13**, 1135-1147; (b) A. M. Lowe, N. L. Abbott, *Chem. Mater.* 2011, **24**, 746-758; (c) P. S. Noonan, R. H. Roberts, D. K. Schwartz, J. Am. Chem. Soc. 2013, 135, 5183-5189; d) S. J. Woltman, G. D. Jay, G. P. Crawford, *Nat. Mater*. 2007, **6**, 929-938.

5 (a) S. Tomar, M. M. Green, L. A. Day, *J. Am. Chem. Soc.* 2007, **129**, 3367-3375; (b) E. Barry, D. Beller, Z. Dogic, *Soft Matter* 2009, **5**, 2563-2570. (c) Z. Zhang, E. Grelet, *Soft Matter* 2013, **9**, 1015-1024.

6 (a) J.-W. Oh, W.-J. Chung, K. Heo, H.-E. Jin, B. Y. Lee, E. Wang, C. Zueger, W. Wong, J. Meyer, C. Kim, *Nature Comm.* 2014, **5**,3034; (b) K. E. Shopsowitz, H. Qi, W. Y. Hamad, M. J. MacLachlan, *Nature* 2010, **468**, 422-425.

7 D. Marvin, R. Hale, C. Nave, M. H. Citterich, *J. Mol. Biol*. 1994, **235**, 260-286.

8 (a) K. Kataoka, H. Miyazaki, M. Bunya, T. Okano, Y. Sakurai, *J. Am. Chem. Soc.* 1998, **120**, 12694-12695; (b) D. Roy, B. S. Sumerlin, *ACS Macro Lett.* 2012, **1**, 529-532.

9 (a) S. D. Bull, M. G. Davidson, J. M. Van den Elsen, J. S. Fossey, A. T. A. Jenkins, Y.-B. Jiang, Y. Kubo, F. Marken, K. Sakurai, J. Zhao, *Acc. Chem. Res.* 2012, **46**, 312-326; (b) X. Wu, Z. Li, X.-X. Chen, J. S. Fossey, T. D. James, Y.-B. Jiang, *Chem. Soc. Rev.* 2013, **42**, 8032-8048.

10 M. L. Stolowitz, C. Ahlem, K. A. Hughes, R. J. Kaiser, E. A. Kesicki, G. Li, K. P. Lund, S. M. Torkelson, J. P. Wiley, *Bioconjugate Chem.* 2001, **12**, 229-239.

11 (a) J. Buitenhuis, *Langmuir*, 2012, **28**, 13354-13363; (b) K. Zimmermann, H. Hagedorn, C. C. Heuck, M. Hinrichsen, H. Ludwig, *J. Biol. Chem.* 1986, **261**, 1653-1655.

12 G. E. Arnold, L. A. Day, A. K. Dunker, *Biochemistry* 1992, **31**, 7948-7956.

13 G. Springsteen, B. Wang, *Tetrahedron* 2002, **58**, 5291-5300.

14 H. Ueno, T. Iwata, N. Koshiba, D. Takahashi, K. Toshima, *Chem. Commun.* 2013, **49**, 10403-10405.

15 (a) Y.-J. Huang, W.-J. Ouyang, X. Wu, Z. Li, J. S. Fossey, T. D. James, Y.-B. Jiang, *J. Am. Chem. Soc.* 2013, **135**, 1700-1703; (b) W. Wu, T. Zhou, A. Berliner, P. Banerjee, S. Zhou, *Angew. Chem.* , *Int. Ed.* 2010, **122**, 6704-6708; (c) Y. Liu, C. Deng, L. Tang, A. Qin, R. Hu, J. Z. Sun, B. Z. Tang, *J. Am. Chem. Soc.* 2010, **133**, 660-663.